Accepted Manuscript

Preparation of ibuprofen microparticles by anti-solvent precipitation crystallization (APC) technique: characterization, formulation and in-vitro performance

Afrina Afrose, Edward T. White, Tony Howes, Graeme George, Abdur Rashid, Llew Rintoul, Nazrul Islam

PII: S0022-3549(18)30497-0

DOI: 10.1016/j.xphs.2018.07.030

Reference: XPHS 1242

To appear in: *Journal of Pharmaceutical Sciences*

Received Date: 5 June 2018

Accepted Date: 31 July 2018

Please cite this article as: Afrose A, White ET, Howes T, George G, Rashid A, Rintoul L, Islam N, Preparation of ibuprofen microparticles by anti-solvent precipitation crystallization (APC) technique: characterization, formulation and in-vitro performance, *Journal of Pharmaceutical Sciences* (2018), doi: 10.1016/j.xphs.2018.07.030.

Preparation of ibuprofen microparticles by anti-solvent precipitation crystallization (APC) technique: characterization, formulation and in-vitro performance

Afrina Afrose[1,2], Edward T White[3], Tony Howes[3], Graeme George[2,4], Abdur Rashid[5], Llew Rintoul[4], and Nazrul Islam[1,2,*]

[1]Pharmacy Discipline, School of Clinical Sciences, Faculty of Health, Queensland University of Technology, Brisbane, QLD

[2]Institute of Health and Biomedical Innovation, Queensland University of Technology, Brisbane, QLD

[3]School of Chemical Engineering, The University of Queensland, Brisbane, QLD.

[4]School of Chemistry, Physics and Mechanical Engineering, Science and Engineering Faculty, Queensland University of Technology, Brisbane, QLD

[5]Md Abdur Rashid, Assistant Professor, Department of Pharmaceutics, School of Pharmacy, King Khalid University, Guraiger, Abha-62529, Kingdom of Saudi Arabia.

** The corresponding author*

Dr. Nazrul Islam

Pharmacy Discipline, School of Clinical Sciences, Faculty of Health, Queensland University of Technology, Brisbane, QLD.
E-mail: nazrul.islam@qut.edu.au
Phone No. +61 07 31381899

Abstract

This study demonstrates the preparation and characterization of ibuprofen (IBP) microparticles with some excipients by a controlled crystallization technique with improved dissolution performance. Using the optimum concentrations Pluronic F127 (Pl F127), hydroxypropyl methyl cellulose (HPMC), D-mannitol and L-leucine in aqueous ethanol, the IBP microparticles were prepared. The dissolution tests were performed in phosphate buffer saline (PBS) using a USP dissolution tester at 37°C. The Raman spectroscopy was used to investigate the interactions and distribution of the IBP with the additives in the microcrystals. The prepared IBP microparticles showed higher dissolution compared to that of the smaller sized original IBP particles. The Raman data revealed that the excipients with a large number of hydroxyl groups distributed around the IBP particle in the crystal, enhanced the dissolution of the drug by increasing the drug-solvent interaction presumably through hydrogen bonding. The Raman mapping technique gave an insight into the enhanced dissolution behaviour of the prepared IBP microparticles and such information will be useful for developing pharmaceutical formulations of hydrophobic drugs. The controlled crystallization was a useful technique to prepare complex crystals of IBP microparticles along with other additives to achieve the enhanced dissolution profile.

Key words: Ibuprofen, crystallinity, Raman mapping, excipients, dissolution.

1. Introduction

Antisolvent precipitation crystallization (APC) of particles is a technique that provides the framework for an appropriate design of micro/nanoparticles to produce engineered particles with desired physicochemical properties to meet the requirements in their practical applications[1]. Addition of additives such as mannitol (morphology modifier, discrete particle former), leucine (dispersibility enhancer), pluronic (crystal size inhibitor) and hypromellose (HPMC, as crystal/agglomerate growth inhibitor) in crystallizing drug particles have been studied [2-7]. Using Ibuprofen (IBP) as a model drug, this study attempted to prepare IBP micro/nanoparticles with these additives for their characterization and to understand the impact of these excipients in the formation and dissolution performances of the active drug.

Ibuprofen, a non-steroidal anti-inflammatory drug, is used as various dosage forms in the treatment of various diseases. This drug is poorly water soluble and thereby the rate of dissolution from the currently available dosage forms are limited that leads to poor bioavailability at high dose. Despite the fact that the IBP is a commonly used high dose therapeutic medicine, its poor solubility in aqueous solutions lessens the dissolution and absorption rates [8]. Crystals of IBU prepared by conventional methods and subsequent micronization by milling are very difficult to reduce in particle size for improving the solubility. Dry milling is a commonly used technique to reduce particle size and most of the time particles tend to deform rather than fragment during the milling process. The heat generated during dry milling cause partial melting (as this drug has a low melting point) of the milled particles and thereby produce a large number of amorphous particles that tend to form large agglomerates [9]. The conventional micronization process (i.e. milling, homogenization) with high energy input incorporates undesirable particle shape, size, surface charge modifications, and decreased crystallinity that affect the physicochemical properties.

Raman microscopy, a non-destructive analytical technique is used in pharmaceutical product design for visualization of component distribution in dosage forms[10,11] such as tablets[12], solid dispersion[13] and powder mixtures[14]. Our study demonstrates an anti-solvent crystallization

process for the preparation of IBP microparticles with some excipients (HPMC, mannitol, leucine and pluronic) to understand their distribution in the microcrystals and subsequent dissolution behaviour of the active drug. In this study, we utilized Raman Micro-Spectroscopy for mapping of the individual excipients in a powder mixture to identify the distribution of active drug among other additives, and their effects on the dissolution of the IBP from the prepared microcrystals.

2. Material and methods

2.1 Materials

Ibuprofen (IBP) was used as the active pharmaceutical ingredient in this study. USP grade IBP (Part no: 30-1192-1000GM) was purchased from Professional Compounding Chemists of Australia Pty Ltd (PCCA, Matraville, NSW 2036), as a high purity racemate of (R)/(S)-(±)-[2-(4-isobutyl-phenyl) propionic acid] with the empirical formula $C_{13}H_{18}O_2$ and molecular weight 206.27. Pluronic F127 (Pl F127) is a surfactant copolymer (Poloxamer 407 NF, Part no: 302637-500GM) and was purchased from PCCA (Matraville, NSW). Hydroxypropyl methyl cellulose/ hypromellose (HPMC), used as stabilizer was purchased from Sigma-Aldrich (09963-100 G, Lot: BCBG6002V). D-mannitol ($C_6H_8OH_6$), used as a cryoprotectant and bulking agent was purchased from Sigma-Aldrich (Part No: M4-125-500 g, Lot no: SLBJ5312V). L-Leucine ($C_6H_{13}NO_2$) (Bioultra, ≥ 99.5%), an amphiphilic surfactant used as a dispersive adjuvant was purchased from Sigma-Aldrich (Part No: 61819-100 G, Lot No: BCBM2322V). Spectrophotometric grade ethanol was purchased from Sigma-Aldrich and deionised/Millipore water is available in the laboratory. All the materials were used as received.

2.2 Methods

2.2.1 Preparation of HPMC solutions

Solutions containing 5% w/w HPMC were prepared by adding HPMC powder to a weight of water required to make up to one tenth of the final weight. Vigorous agitation was used until the powder was dissolved. The solution was then refrigerated for 24 hours at 4°C to allow polymer hydration, made up to final weight and stored refrigerated for 72 hours prior to use [15]. The final solvents of the required concentration of additives were prepared by taking the weighed amount of Pl F127, leucine and mannitol powder, made up to the final weight with the 5% HPMC solution and water/aqueous ethanol to give the additives in the concentration range

HPMC 0-0.8%, Pl F127 0-1.8%, leucine 0-1.5% and mannitol 0-9%. They were magnetically stirred until complete dissolution was observed.

2.2.2 Anti-solvent precipitation crystallization (APC) method for particle preparation

The method for particle preparation was the anti-solvent precipitation crystallization (APC) by a co-solvent technique [16]. This technique involves mixing of two different phases as demonstrated in Fig. 1. The first phase (solvent phase) is ethanol with dissolved IBP (30-200 mg/g) depending on the batch size. The second phase (anti-solvent phase, water) in which IBP is practically insoluble contains the dissolved additives**.** The crystallizer comprises an ultrasonic bath (Soniclean 750 HT), the cooler (Julabo, FT 200), the constant temperature heating immersion circulator ED (Julabo) and the overhead stirrer (Lab Co.).Various process parameters (Table 1) including temperature, concentration of excipients (HPMC, Pl F127, leucine and mannitol), batch size, use of ultrasound and stirring speed were varied to get the best size of the micro/nanocrystals. The compositions of the prepared particles formulations are given in Table 2.

2.2.3 Freeze drying process for particle recovery

The micro/nano crystal product suspensions were centrifuged at 3500 rpm for 60 minutes in Falcon tubes (10ml and 50ml) to remove non-adhering additives. The excess liquid was discarded and the remainder was frozen using a deep freezer at -75ºC for 24 hours. These frozen semisolids were freeze dried using a lyophilizer (Alpha 1-4 LD plus) at a temperature of -55°C and vacuum 1.0 mbar absolute for 24 – 96 hours, depending on the sample volume.

2.2.4 Particle size reduction by mill micronizer

A McCrone Micronizing mill was used to mill raw IBP powder down to the similar size obtained by controlled crystallization technique. Raw IBP powder was loaded (< 3 g) into the micronizer vessels with zirconia beads. Water with > 300 ppm of detergent (2 mL) was used as a fluid. Particles with the required size were found after 12 hours of milling. The samples were then dried in an oven overnight at 40 °C.

2.3. Characterization of prepared particles

2.3.1. *Density and flow property measurements*

The density, angle of repose, Carr's index and the Hausner ratio of the prepared IBP crystals was determined by the methodology published elsewhere [17]. Using the Erweka tapped density tester, the densities of powders were determined. After observing the initial powder volume and mass, the graduated 5 mL measuring cylinder was mechanically tapped, and volume readings were taken until no further volume change was observed. A 5 mL graduated cylinder was filled with a mass of 1.3 ± 0.3 g of powder sample. Then the cylinder was secured in the support of the tapping apparatus and 100, 500 and 1250 taps on the same powder sample were carried out, and the corresponding volumes V_{100}, V_{500} and V_{1250} were recorded to the nearest graduated unit. In this work, the Carr's index and Hausner ratio was calculated using measured values of bulk density (ρ_{bulk}) and tapped density (ρ_{tapped}) as follows:

$$Carr's\ Compressibility\ index = 100 \times \frac{\rho_{tapped} - \rho_{bulk}}{\rho_{tapped}} \quad (1)$$

$$Hausner\ Ratio = \frac{\rho_{tapped}}{\rho_{bulk}} \quad (2)$$

The flowability of the samples was determined using the generally accepted scale of flowability for the Carr's index and the Hausner ratio[18]. Measurements were taken from three replicates of each of the formulations.

2.3.2. *Angle of repose*

To form the angle of repose on a fixed base, a 5 mL beaker was used as a base (10 mm diameter) to retain the powder (250 ± 0.5 mg). The powder was poured through a funnel (40 mm diameter and 65 mm height). The funnel height was maintained at approximately 2 – 4 cm from the top of the powder pile which is formed in order to minimise the impact of falling powder on the tip of the cone. The angle of repose was determined by measuring the height of the cone of powder and calculating the angle of repose, α, from the following equation:

$$\tan(\alpha) = \frac{height}{0.5 \times base} \quad (3)$$

The degree of flowability was determined from the flow properties corresponding to the angles of repose[17]. Measurements were taken from three replicates of each of the formulations.

2.3.3. *Particle size measurement*

The particle size of the crystallized IBP was measured by the laser diffraction technique using a Malvern Mastersizer 3000 equipped with a small volume dispersion unit. It is estimated that the relative error in the volume median diameter (VMD) calculated by the Malvern Mastersizer is ± 2% [19]. Particle size measurements for the finer nanocrystals were done using the Zetasizer (NanoZS 90, Malvern Instruments, UK). The suspending media was the saturated IBP solution prepared with an equivalent composition to the final crystallization media at equilibrium. This media was used as the dispersant in the Malvern 3000 small volume (120 ml) dispersion unit stirring at 2000 rpm. A small amount of prepared powder was dispersed in 5.0 mL of this dispersion media and sonicated for 5 minutes to ensure all particles dispersed in the suspension. Few drops of this concentrated suspensions was added dropwise in the dispersion unit until the obscuration reached the desired level. The refractive indexes used for IBP and the dispersant were 1.43 and 1.33, respectively. The absorption index was 1.2. The mass median diameter (MMD, D[v,0.5]) and volume mean diameter (D [4,3]) determined from the output of the laser diffraction particle sizing were used as the major size parameter to characterize the particle size distributions (PSD). Measurements were taken from three replicates of each of the formulations.

2.3.4. *Scanning electron microscope (SEM)*

A Zeiss Sigma scanning electron microscope was used to investigate the morphological properties (shape, size and surface) of the IBP crystals. The sample preparation involved fixing the powder samples on to a metal stub with the aid of a double sided adhesive tape followed by coating for 180 seconds with a LEICA EM SCD005 gold coater. Scanning electron microscopy (SEM) was then carried out by loading the sample on the SEM working at 5 KV.

2.3.5. Drug loading determination

Quantification of the IBP content in the powder formulation was determined by UV spectrophotometer (Thermo Scientific Evolution Array) at a wavelength of 264 nm. Samples were prepared by dissolving a known 10-15 mg of powder formulation in a known 10 (± 1) g of 50% aqueous ethanol solvent system. Complete solution of IBP in the selected solvent system was confirmed from the predetermined solubility results.

2.3.6 Differential scanning calorimetry (DSC)

Differential scanning calorimetry (DSC) experiments were carried out in a DSC Q100 from TA Instruments Explorer Q series. A known small amount of sample (<6 mg) was enclosed in a hermetic sealed aluminum pan. A liquid nitrogen cooling system was used in order to reach temperatures as low as - 42 °C. Processed and unprocessed IBP samples were scanned from 10 °C to 110 °C, using a heating rate of 10°C/min. All samples were analysed in triplicate. The percent crystallinity is determined using equation 4:

$$\% \text{ Crystallinity} = \Delta H_m / \Delta H_m^\circ \times 100\% \qquad (4)$$

The heats of melting, ΔH_m, determined by integrating the areas (J/g) under the peaks using TA instrument Analysis 2000 software. The term ΔH_m° is a reference value and represents the heat of melting of the 100% crystalline IBP. It was found that the melting enthalpy of the raw IBP powder was 118.4 ± 7.3 J/g which is also in agreement with Nokhodchi and co-workers [3]. This value was used as the reference value to determine the percentage crystalline phase of IBP in the processed formulations with different compositions of additive.

2.3.7. Powder X-ray diffraction (XRD)

The crystallinities of the unprocessed and processed IBP were evaluated using an X-ray powder diffractometer (XRD). Samples were front pressed into low background quartz holders. Diffraction patterns were collected in θ/2θ geometry on a PANalytical X'Pert Pro diffractometer (Co Kα) using a W/Si parabolic mirror and 0.09° collimator before the point detector. A 0.25° fixed divergence slit, 10 mm mask, 1.4 mm incident anti-scatter slit, and 0.04 rad pre and post diffraction Soller slits were used. Patterns were collected from 3 – 75° 2θ at a step size of 0.02° for 1 hr. The sample was spun during data collection. An instrument function was determined from LaB_6 (SRM 660a). Phase identification was performed with Highscore Plus (V4.5, PANalytical) using the PDF4+ database (ICDD) and confirmed via Rietveld refinement with TOPAS (V5, Bruker). Quantitative phase analysis was performed using TOPAS (v5, Bruker) via the Rietveld method. An instrument function determined from LaB6 (NIST SRM 660a) was used to model the profile shape. A Lorentzian crystallite size term was refined for each phase to account for profile broadening. Refined terms included specimen displacement, scale factor for each phase, and unit cell parameters for each phase. The amount of Pl F127 in some samples was estimated by the degree of crystallinity method where the numerical area of each phase is used to

determine abundances. The Pl F127 was accounted for by modelling a peak at ca. 27° 2θ (most obvious feature not modelled) and designating it as the amorphous phase. HPMC phase abundance could not be quantified as its concentration in the formulation was too low to identify in the XRD curves. XRD patterns of both the processed and unprocessed IBP were compared to identify any alteration in their crystallinities.

2.3.8. Raman spectroscopy

A WITec Alpha 300 series Raman Microscope equipped with a 532 nm laser was used for spectral analysis of the individual components and the powder formulations. The purpose of the analysis was to identify the IBP component and additives and their distribution by recording Raman maps over selected regions of the powder formulations. To prepare the sample for mapping a stainless steel cup was piled slightly high with the formulation powder, which was then lightly tamped down by placing a coverslip over the top of the cup. The purpose of the coverslip was to establish a horizontal region in the sample that would remain in focus over the region to be studied. Raman maps were measured by rastering in the horizontal plane in 0.5 μm increments over a 20 x 20 μm region of the powder with the focal plane of the microscope set to just beneath the coverslip. Spectra were recorded at each increment with the integration time of 1s and a laser power of 10 mW. The Raman microscope was calibrated to the 520.5 nm line of a silicon wafer. The Zeiss 50× objective with a 0.7 NA used forms a confocal sample volume approximating a cylinder of 0.5 μm diameter and 2-3 μm high. The mapping of the powder components in the mixture and the spectral analysis including CLS calculations were performed using WITec Control Four and Project Four software.

2.3.9. In vitro drug dissolution test

The USP paddle method (Pharma Test- DT 70) was adopted in 900 mL phosphate buffered saline (PBS, pH 7.4) at 100 rpm and 37 °C for each sample. At the fixed time intervals of 2, 6, 10, 15, 20, 30, 60, 90 and 120 minutes, 5 mL aliquots of the release medium were withdrawn and the same amount replaced with the fresh PBS. The drug content in the withdrawn aliquot was analyzed by UV spectrophotometry at 221 nm. Percentage drug release versus time data were

plotted to establish drug release profiles from the formulations. Three replicates were undertaken on each sample. A sample of milled pure IBP (12.5 mg; size 2.8 ± 0.1 µm) used as the control and three processed formulations (F4, F6 and F10, Table 2) equivalent to 12.5 mg of pure IBP were selected for dissolution studies as these processed formulations showed better flow property.

2.3.10. Statistical analysis: All statistical analysis was performed using Microsoft Excel (2016).

3. Results and discussions

3.1 Formulations of the prepared particles

To evaluate the efficiency of the processed IBP powder in an APC process, 14 different formulations were prepared based on the different batch size of crystallization, initial IBP concentrations and additive concentrations. It is noted that the additives mentioned in Table 2 are the percentages that were dissolved in the crystallization medium for the total batch size and are not the additive contents of the crystal product. Each of the products from these formulations was characterized for density, flowability, particle size distribution, morphology, and crystallinity. F1, F2, F3, F6 and F7 formulations had different batch sizes from the usual 50g. IBP concentration was varied from 0.3% to 2% in the formulations F1 to F6. Additive concentrations (Pl F127, HPMC, L-leucine and D-mannitol) were varied in other runs. Initially, using different batch size (10-50 g) the precipitation experiments were carried out at various stirring speeds (500-2000 rpm) with different duration of mixing (30-60 minutes) to produce small particles. Based on the initial runs (a large number of raw data are not presented in this article), the best parameters were selected to produce reproducible particle size from a fixed batch of the formulation containing the fixed amounts of different components. Finally, keeping the constant solvent-anti-solvent ratio (1:9), the optimized process parameters demonstrated in Table 1 have been selected from these initial studies for the rest of the experiments with varying concentrations of other excipients as demonstrated in Table 2 to obtain similar particle size presented in Table 3.

3.2 Particle size & size distribution

Particle size and size distribution of the prepared IBU crystals are presented in Table 3. The size of particles was affected by the presence of different concentrations of surfactant Pl F127. The decrease in size occurred with increased concentration of Pl F123 until 1.2% (F7) in the formulations; however, the size increased at 1.8% of Pl F127 (Formulation 9; Suppl Fig. S1). Both mannitol and PL F127 aid in reducing particle size. FPO and FMO are the formulations without Pl F127 and D-mannitol respectively, and particles grew larger in these formulations due to their absence. The literature has shown that mannitol prevents nanoparticle aggregation during the drying process. The stabilization of particles during the freeze drying is proposed to occur by sugars isolating individual particles in the unfrozen fraction, thereby preventing aggregation during freezing above the glass transition temperature, T_g [20]. In this case, the transition of the substance into a glass is not required for this effect and the spatial separation of particles within the unfrozen fraction is sufficient to prevent aggregation[20]. As a result, the particle size was expected to remain stable with no further growth due to aggregation after the drying step.

3.3 Density, angle of repose & flowability

The estimation of the bulk density and tapped density (resulting in the Carr's index and Hausner ratio) and also the angle of repose for estimating flowability are given in Table 4. Flowability of all the formulations was determined and the effect of the additive and drug concentration on it was observed from the obtained results. The purpose of preparing all of these formulations was to identify those formulations with smaller particle size for faster dissolution. Table 4 shows that formulations F3, F4, F6, F10 and FMO had good flow properties (Angle of Repose, AR): 31-35; Carr's index (CI): 11-15; Hausner ratio (HR): 1.12-1.18), F1, F2 and FLO were passable and the rest were poor (Table 4). Of those with good or passable flowabilities; the FPO and FMO formulations had larger particle size (D[4,3] > 10 μm) compared to others. It was expected that the additive concentration might have a significant effect on the flow properties of the prepared IBP particles due to their hygroscopic nature. L-leucine is a well-accepted dispersive excipient for use in pharmaceutical formulations and it has been found to improve the powder flowability in several cases due to its anti-adhesive [21,22] functions and surfactant properties [2,23]. Hence, to see the leucine effect on flowability, its concentration was increased gradually from 0%, through 0.9%, 1.2% to 1.5% in FLO, F7, F10 and F11 formulations, respectively. However, no specific

trend was observed in the flowability according to the values of Carr's index, Hausner ratio and angle of repose (as illustrated by the angle of repose, Table 4). Surprisingly, FLO has no leucine but showed a better flowability than those of the formulations containing 1.5% leucine (F7 and F11). An optimal amount of leucine is critical to achieving the desired properties of the leucine coated particles, as excessive leucine decreases stability with no additional benefits [24]. Interestingly, an increase in the Pl F127 concentration in the formulations FPO, F8, F7 and F9, where concentration of PL F127 was increased from 0% to 0.6%, 1.2% and 1.8%, appeared to influence the flowability negatively. A possible reason could be the decreased particle size with increasing Pl F127 concentration, caused the flowability to decrease [25]. It has been reported that the drug particle has a partial amorphous form due to the presence of Pl F127 [26], which might have influenced the powder flow negatively. Thus, although leucine has remarkable effects, other excipients used to prepare the IBP microparticles have no such effect on the flowability of the prepared powders.

3.4 Particle Morphology by SEM

The particle morphology of the formulations was investigated by scanning electron microscopy (SEM). The SEM images of raw IBP, milled raw IBP and all the formulations are presented in Fig. 2. The crystal habit of IBP depends on the crystallization conditions such as the solvent type and presence of additives[2,27]. The SEM images show that the commercial raw IBP is needle-shaped, whereas the particles crystallized in the presence of various additives are mostly of irregular shapes with pores in the agglomerates. In the case of formulation F5, the crystallization was carried out in the absence of leucine and mannitol, which resulted in a different morphology, with the crystals having rough surfaces comprising flat-shaped IBP particles sticking together to make bigger particles. As the SEM images represent the dried form of formulation, it is very likely the particles in F5 formulation aggregated/ agglomerated into large irregular shapes due to drying without the leucine and mannitol. The morphology of the formulations F6, F7, F8, F9, F10, F11, FPO, FLO and FMO with low IBP concentration (0.3%) seems to be the agglomerates of IBP microparticles adhering to each other. The IBP particles in FMO are seen clearly in the tight agglomerated form of chunky shaped crystals. The images revealed that the needle shaped crystals actually represents the crystal habit of D-mannitol in the

powder mixtures. However, the IBP particle morphology was significantly influenced by both the additive composition and concentration.

3.5 Raman mapping for excipients distribution in the microcrystals of IBP

The particle morphology was investigated using Raman spectroscopy to identify each component individually and the distribution of the drug particle with the additives in the powder mixture is represented in Fig. 3. Image A is formed by merging the component images to give an overall impression of distribution of all components in the co-crystal. The individual components such as red representing leucine (B); magenta-pluronic F127 (C), green-HPMC (D), yellow-IBP (E), and aqua-mannitol (F) are also shown. The Raman images revealed that IBP drug particles are surrounded by the additives used. The distribution of Pl F127, HPMC and L-leucine around the IBP particle, reflected the interactions of those excipients with the active drug during the APC process.

To explore the possible associations between the excipients and IBP, correlation diagrams were prepared by plotting the relative concentration of each component vs the IBP concentration for each mapped point. Results are only shown for those points where significant IBP was present. Correlation plots for the representative formulation F6 are given in Figs. 4 (A-D). A broad trend to higher leucine corresponding to higher IBP concentrations seen in Figs 4A suggesting a positive correlation between the relatively hydrophobic components leucine and IBP. The Pl F127 is closely associated with IBP without significant correlation (4B). The presence of hydrophilic HPMC (4C) is poorly distributed in regions of high IBP, suggested a negative correlation between the cellulose components with extremely hydrophobic IBP. However, the hydrophilic mannitol (4D) is distributed in the region of high IBP and very closely associated with the drug particle presumably due to hydrogen bonding. These outcomes helped get a clear understanding on the solubility/dissolution behavior of the prepared IBP microcrystals.

3.6 Crystallinity

The crystallinity of the raw IBP powder, milled IBP powder, additives and the powder formulations was examined using differential scanning calorimetry (DSC). The DSC data are presented in Figs. 5 A & B). All the formulations produced an endothermic peak in the range of 74–78°C, which are in agreement (within ± 2.0 °C) with the previous reports which suggest that

IBP exists as crystalline solid exhibiting a typical melting range of 75–77 °C; however, the melting point of pure IBP is 77.5ºC[28]. The melting point for pure IBP, HPMC, Pl F127, mannitol and leucine had shown a sharp peak before the melting point of the pure IBP drug (Fig. 5A). The additive melting peaks confirmed that the presence of mannitol and leucine would not interfere with the pure IBP melting peak identification in DSC, but HPMC and Pl F127 could. Fig. 5B represents the DSC curves for raw and milled IBP and all the prepared formulations where the endothermic peaks for all the formulations, within the melting point range for pure crystalline IBP; however, the height of the peaks changed with respect to the IBP content in the formulations. The pure, milled IBP particle and formulations with high concentrations of IBP (F4 and F5) showed very sharp peaks, whereas the crystals with other additives and low concentrations of IBP showed smaller and broader peaks suggesting that the IBP in the prepared formulations are both in crystalline and amorphous forms. The pure IBP showed 100% crystallinity, milled IPB produced 94.7% crystallinity due to crushing; however, formulations (F4 and F5) with 2.0% IBP at varying concentrations of other excipients showed 96-99% crystallinity (Suppl Table S1). Other formulations with low concentrations of IBP in presence of other excipients at varying concentrations produced more or less 50% amorphous particles.

3.7 Dissolution studies

The dissolution profile of the milled raw IBP powder was much slower compared to those of the prepared formulations (Fig. 6). Theoretically, it was expected that the smallest particle size of the milled ibuprofen (2.8µm, Table 3) compared to the prepared particles would have a higher surface area which could enhance the solubility. However, this did not happen presumably due to the strong hydrophobic nature of the drug particle. The prepared IBP micropartilces showed faster drug release/dissolution (Fig 6). It can be noted that the drug release from F4, F6 and F10 were 56, 64 and 96%, respectively in first two minutes. The results indicated that the dissolution rate of the prepared formulations was significantly faster than that of the milled pure IBP (<50% in 2 minutes). The formulations with the higher initial IBP and lower additive concentrations have shown a comparatively lower dissolution rate in the first two minutes. Formulation F10 showed the highest drug release (96%) in the first two minutes. The possible reason could be the presence of a higher content of additives (Pl F127 1.2%, L-leucine 1.2%, D-mannitol 9.0% and HPMC 0.2%, Table 2) and very low initial drug load (0.3%) in the formulation F10 which

favoured the dissolution process by decreasing drug-drug cohesion and increasing the drug-solvent interaction. The Raman images (Fig. 3) clearly demonstrated that a large number of excipients especially the amphiphilic leucine and hydrophilic HPMC and D-mannitol containing a large number of hydrophilic hydroxyl groups are distributed around the IBP particle in the microcrystals. This suggests that the hydroxyl groups of these excipients enhanced the dissolution of the drug by increasing the drug-solvent interaction. The hydrophilic HPMC (Fig. 4C) is poorly associated in regions of extremely hydrophobic IBP. However, because of the amorphous character and extensive hydrogen-bonded network, it may help increase the dissolution by interacting with solvent through hydrogen bonding. In contrast, the hydrophilic mannitol (Fig. 4D) is closely associated with IBP which presumably led to the enhanced dissolution by hydrogen bonding.The enhanced dissolution of the prepared formulations especially the formulation F4 indicated that the presence of the hydrophilic surfactant pluronic (Fig. 4B) around the IBU particles (Fig. 3 E) strongly promoted drug wettability by reducing the surface tension of the hydrophobic IBP particles. Additionally, the presence of amphiphilic surfactant L-leucine in the complex crystal played a significant role in increasing dissolution of the drug possibly due to the orientation of hydroxyl groups towards the aqueous solvent, which increased the particle-solvent interactions and improved the dissolution process[29]. The presence of hydrophilic surfactant pluronic and amphiphilic leucine around the IBP crystal strongly promoted the wettability by reducing the surface tension of the hydrophobic IBP particles leading to increased dissolution. Additionally, the amorphous IBP particles in the prepared formulations especially the sample F6 (52% crystalline, Suppl Table S1) containing the low concentration of IBP (1.0%) showed higher dissolution (Fig. 6), as this particle in the amorphous state contained limited crystal lattice interactions or bonds that needed to break for the drug to enter solution leading to higher dissolution compared to that of the pure crystals, which has greater intermolecular forces in the crystal. Furthermore, the formation of pores in the complex microparticles (SEM images Figs 2) increased the surface area and wettability of drug particles and led to increasing the solubility/dissolution. On the other hand, the relatively higher cohesive forces among the milled pure IBP particles with the smallest size (2.8µm) potentially influenced the overall dissolution negatively due to the extreme hydrophobic nature[30]. The maximum release from milled pure IBP was 71%, whereas, from the prepared formulations F4, F6 and F10

were 100, 87% and 96%, respectively in 20 minutes. This promising outcome of dissolution studies of the prepared microcrystals ensured the superiority of the prepared IBP over pure milled drug particles. Therefore, it can be emphasized that the prepared formulations are better than the milled IBP in terms of the dissolution behaviour. The faster dissolution performance of the prepared powder formulations would be useful for the development of dosage forms like tablet, capsule, suspensions, and formulation for inhalation to achieve an improved bioavailability.

4. Conclusion

This study reports the preparation of the hydrophobic IBP microparticles along with other additives (HPMC, mannitol, leucine and pluronic) by a controlled crystallization technique with enhanced dissolution profile. The prepared IBP microparticles showed higher dissolution compared to that of the smaller sized original milled IBP particles as the presence of hydrophilic excipients in the formulation played a vital role. The Raman spectroscopy used for the first time in this study to investigate the interactions and distribution of the IBP with other additives present in the microcrystals, clearly demonstrated that a large number of excipients especially the amphiphilic leucine and hydrophilic HPMC and D-mannitol containing a large number of hydrophilic hydroxyl groups are distributed around the IBP particle. The hydroxyl groups of these excipients enhanced the dissolution of the drug by increasing the drug-solvent interaction. The hydrophilic HPMC and mannitol associated in regions of extremely hydrophobic IBP in the in the microcrystals, they presumably increase the dissolution process by interacting with solvent through hydrogen bonding. The Raman mapping technique, which provides the distribution of different components in the microcrystals, gave an insight into the enhanced solubility/dissolution behaviour of the prepared IBP microparticles. Such information will be useful for developing pharmaceutical formulations with better solubility and dissolution properties of hydrophobic drugs.

Acknowledgement: The authors gratefully acknowledge the financial support of PhD scholarship for Afrina Afrose from Queensland University of Technology (QUT, Australia. The Raman data reported was obtained using the resources of the Central Analytical Research

Facility (CARF) at the Institute for Future Environments. Access to CARF is supported by generous funding from the Science and Engineering Faculty (QUT).

The authors declare no conflict of interest.

References

1. Ragab D, Rohani S, Samaha MW, El-Khawas FM, El-Maradny HA 2010. Crystallization of progesterone for pulmonary drug delivery. J Pharm Sci 99(3):1123-1137.
2. Kaialy W, Nokhodchi A 2016. The use of freeze-dried mannitol to enhance the in vitro aerosolization behaviour of budesonide from the Aerolizer®. Powder Technol 288:291-302.
3. Nokhodchi A, Homayouni A, Araya R, Kaialy W, Obeidat W, Asare-Addo K 2015. Crystal engineering of ibuprofen using starch derivatives in crystallization medium to produce promising ibuprofen with improved pharmaceutical performance. RSC Advances 5(57):46119-46131.
4. Raula J, Thielmann F, Kansikas J, Hietala S, Annala M 2008. Seppälä J, Investigations on the Humidity-Induced Transformations of Salbutamol Sulphate Particles Coated with l-Leucine. Pharm Res 25:2250-2261.
5. Terebetski JL, Michniak-Kohn B 2014. Combining ibuprofen sodium with cellulosic polymers: A deep dive into mechanisms of prolonged supersaturation. Int J Pharm 475(1-2):536-546.
6. Kumar S, Gokhale R, Burgess DJ 2014. Sugars as bulking agents to prevent nano-crystal aggregation during spray or freeze-drying. Int J Pharm 471(1-2):303-311.
7. Malamatari M, Somavarapu S, Kachrimanis K, Buckton G, Taylor KMG 2017. Preparation of respirable nanoparticle agglomerates of the low melting and ductile drug ibuprofen: Impact of formulation parameters. Powder Technol 308:123-134.
8. Bakhbakhi Y, Alfadul S, Ajbar A 2013. Precipitation of Ibuprofen Sodium using compressed carbon dioxide as antisolvent. Eur J Pharm Sci 48(1-2):30-39.
9. Yuminoki K, Takeda M, Kitamura K, Numata S, Kimura K, Takatsuka T, Hashimoto N 2012. Nano-pulverization of poorly water soluble compounds with low melting points by a rotation/revolution pulverizer. Pharmazie 67(8):681-686.
10. Gordon KC, McGoverin CM 2011. Raman mapping of pharmaceuticals. Int J Pharm 417(1-2):151-162.
11. Paudel A, Raijada D, Rantanen J 2015. Raman spectroscopy in pharmaceutical product design. Adv Drug Deliv Rev 89:3-20.
12. Sasic S 2007. Raman Mapping of Low-Content API Pharmaceutical Formulations. I. Mapping of Alprazolam in Alprazolam/Xanax Tablets. Pharm Res 24(1):58-65.
13. Karavas E, Georgarakis M, Docoslis A, Bikiaris D 2007. Combining SEM, TEM, and micro-Raman techniques to differentiate between the amorphous molecular level dispersions and nanodispersions of a poorly water-soluble drug within a polymer matrix. Int J Pharm 340(1-2):76-83.
14. Fussell AL, Grasmeijer F, Frijlink HW, Boer AH, Offerhaus HL 2014. CARS microscopy as a tool for studying the distribution of micronised drugs in adhesive mixtures for inhalation. J Raman Spectrosc 45(7):495-500.
15. Bajwa GS, Sammon C, Timmins P, Melia CD 2009. Molecular and mechanical properties of hydroxypropyl methylcellulose solutions during the sol:gel transition. Polymer 50(19):4571-4576.
16. Khan S, Matas Md, Zhang J, Anwar J 2013. Nanocrystal Preparation: Low-Energy Precipitation Method Revisited. Crystal Growth & Design 13(7):2766-2777.
17. Lakshmi MGP, Prabha MS, Manikiran SS, Rao NR, J. 2014. Formulation and evaluation of pulsatile salubutamol sulphate tablet in capsule pulsatile release device for asthma. Eur J Biomed Pharm Sci 1(2):125-148.
18. Pharmacopoeia B, Appendix X 2016. Bulk Density and Tapped Density of Powders. British Pharmacopoeia S.

19. Rashid A, White ET, Howes T, Litster JD, Marziano I 2012. Growth rates of ibuprofen crystals grown from ethanol and aqueous ethanol. Chem Eng Res Des 90(1):158-161.
20. Allison SD, Molina MC, Anchordoquy TJ 2000. Stabilization of lipid/DNA complexes during the freezing step of the lyophilization process: the particle isolation hypothesis. Biochim Biophys Acta 1468(1-2):127-138.
21. Islam N, Tuli RA, George GA, Dargaville TR 2014. Colloidal drug probe: Method development and validation for adhesion force measurement using Atomic Force Microscopy. Adv Powder Technol 25(4):1240-1248.
22. Yazdi AK, Smyth HDC 2016. Carrier-free high-dose dry powder inhaler formulation of ibuprofen: Physicochemical characterization and in vitro aerodynamic performance. Int J Pharm 511(1):403-414.
23. Qu L, Zhou QT, Denman JA, Stewart PJ, Hapgood KP, Morton DA 2015. Influence of coating material on the flowability and dissolution of dry-coated fine ibuprofen powders. Eur J Pharm Sci 78:264-272.
24. Ibrahim BM, Jun SW, Lee MY, Kang SH, Yeo Y 2010. Development of inhalable dry powder formulation of basic fibroblast growth factor. Int J Pharm 385(1-2):66-72.
25. Liu LX, Marziano I, Bentham AC, Litster JD, White ET, Howes T 2008. Effect of particle properties on the flowability of ibuprofen powders. Int J Pharm 362(1-2):109-117.
26. Newa M, Bhandari KH, Oh DH, Kim YR, Sung JH, Kim JO, Woo JS, Choi HG, Yong CS 2008. Enhanced Dissolution of Ibuprofen Using Solid Dispersion with Poloxamer 407. Archives Pharm Res 31(11):1497-1507.
27. Nokhodchi A, Amire O, Jelvehgari M, Tehran P 2010. Physico-mechanical and dissolution behaviours of ibuprofen crystals crystallized in the presence of various additives. Daru J Fac Pharm 18(2):74-83.
28. Garekani HA, Sadeghi F, Badiee A, Mostafa SA, Rajabi-Siahboomi AR 2001. Crystal habit modifications of ibuprofen and their physicomechanical characteristics. Drug Dev Ind Pharm 27(8):803-809.
29. Muhsin MDA, George G, Beagley K, Ferro V, Wang H, Islam N 2016. Effects of Chemical Conjugation of L-Leucine to Chitosan on Dispersibility and Controlled Release of Drug from a Nanoparticulate Dry Powder Inhaler Formulation. Mol Pharmaceutics 13(5):1455-1466.
30. Pattnaik S, Swain K, Rao JV, Talla V, Prusty KB, Subudhi SK 2015. Polymer co-processing of ibuprofen through compaction for improved oral absorption. RSC Advances 5(91):74720-74725.

Legend for Figures

Fig. 1. Anti-solvent precipitation crystallization (APC) process for the preparation of IBP microparticles.

Fig.2. Particle morphology of the raw and milled IBP and formulations F1, F2, F3, F4, F5, F6, F7, F8, F9, F10, F11, FLO, FMO and FPO in scanning electron microscopy (Magnification: 5.00 K X).

Fig.3. Raman images of the microcrystal (A) of a representative formulation F6 with the individual components separately coloured: Red for leucine (B); magenta for pluronic F127 (C), green for HPMC (D), yellow for IBP (E), and aqua for mannitol (F). These images demonstrate the way that the drug crystal is surrounded by the excipients.

Fig. 4. Raman correlation plots of formulation F6. A) leucine vs IBP; B) Pl F127 vs IBP; C) HPMC vs IBP; and D) mannitol vs IBP.

Fig. 5. DSC curves for (A) Pluronic F127, HPMC, L-leucine, D-mannitol, raw IBP; (B) milled IBP, F1, F2, F3, F4, F5. F6, F7, F8, F9, F10, F11, FPO, FLO, FMO and raw IBP.

Fig. 6. In vitro dissolution of milled raw IBP powder and some formulations prepared by APC process.

Supplementary Figure

Fig. S1. The effect of Pl F127 concentration on particle size. The crystallization solution contains 0.3% IBP;0.2% HPMC; 0.9% leucine; 9.0% mannitol; 50 g batch (except F7 which was 10 g).

Tables

Table 1: Anti-solvent precipitation crystallization (APC) process parameters and optimized range of conditions for preparing respirable IBP particles.

Process parameters	**Condition**
Batch size	10 – 50 g
Solvent-anti-solvent ratio (solv/anti-solv)	1 : 9 (fixed)
Stirring speed, rpm	600 - 1200
Temperature	25 - 30°C
Ultrasound application	50Hz, max. pulse swept power 180W
Duration of mixing	30 - 60 minutes
Drug concentration in organic phase	0.3-2%
Pl F127 concentration	0-1.8%
HPMC concentration	0-0.8%
Leucine concentration	0-1.5%
Mannitol concentration	0-9%

Table 2. Composition of the different formulations and the amount of additives.

Formulation name	Batch size, g	IBP* conc.%	Leucine*,%, (w/w)	Mannitol*,%, (w/w)	HPMC*,%, (w/w)	Pl F127*,%, (w/w)	Drug loading (%)
F1	10	1	1.3	4.5	0.4	1.8	72.7
F2	30	1	0.9	4.5	0.7	1.3	77.9
F3	10	1	0.9	4.5	0.7	1.3	90.3
F4	50	2	1	8.4	0.1	0.9	99.8
F5	50	2	0	0	0.1	0.9	100.0
F6	10	1	0.9	4.5	0.6	1.2	83.3
FPO	50	0.3	0.9	9.0	0.2	0	84.7
F7	10	0.3	0.9	9.0	0.2	1.2	53.2
F8	50	0.3	0.9	9.0	0.2	0.6	74.6
F9	50	0.3	0.9	9.0	0.2	1.8	43.9
FLO	50	0.3	0	9.0	0.2	1.2	83.9
F10	50	0.3	1.2	9.0	0.2	1.2	73.5
F11	50	0.3	1.5	9.0	0.2	1.2	52.7
FMO	50	0.3	0.9	0	0.2	1.2	99.9

*These are the percentages of drug/additives in total amount of crystallization batch size. F1 to F11 are the formulations with different components. FPO represents the formulation without pluronic, FLO represents the formulation without leucine, and FMO indicates the formulation without mannitol.

Table 3: Particle sizes and distributions of various IBP formulations (units µm± SD, n=3).

Formulation	D[v,0.1]	D[v,0.5]	D[v,0.9]	D[4,3]
F1	2.9 ± 0.1	6.9 ± 0.1	20.4 ± 2.9	9.6 ± 0.8
F2	3.5 ± 0.1	8.5 ± 0.1	18.0 ± 0.2	9.7 ± 0.1
F3	4.6 ± 0.1	17.1±0.5	47.9 ± 1.4	22.0 ± 0.4
F4	3.3 ± 0.6	6.2 ± 0.2	9.3 ± 0.3	6.3 ± 0.2
F5	4.2 ± 0.3	7.2 ± 0.5	11.3 ± 1.5	7.5 ± 0.5
F6	2.9 ± 0.5	5.9 ± 0.8	10.7 ± 1.6	6.5 ± 1.1
FPO	6.1 ± 0.1	11 ± 0.6	18.7 ± 1.3	12.34 ± 1.2
F7	1.1 ± 0.1	3.9 ± 0.4	9.0 ± 0.9	5.1 ± 0.9
F8	3.7 ± 0.1	6.8 ± 0.1	11.9 ± 0.1	7.4 ± 0.1
F9	1.3 ± 0.1	6.1 ± 0.1	12.8 ± 0.3	6.7 ± 0.1
FLO	3.2 ± 0.1	6.1 ± 0.1	10.1 ± 0.3	6.6 ± 0.6
F10	1.4 ± 0.2	6.4 ± 0.3	12.9 ± 0.5	7.1 ± 0.2
F11	1.2 ± 0.0	5.4 ± 0.6	11.8 ± 0.7	6.4 ± 0.4
FMO	3.7 ± 0.1	8.7 ± 0.1	28.2 ± 1.2	20.9 ± 1.3
Milled IBP	1.2 ± 0.1	2.8 ± 0.1	4.45 ± 0.2	2.8 ± 0.1

Table 4: Powder flow properties obtained from different formulations (Mean ± SD, n=3)

Formulation	Bulk density (g/ml)	Tapped density (g/ml)	Carr's index (%)	Hausner ratio	Angle of Repose (°)	Flowability
F1	0.28 ± 0.02	0.36 ± 0.03	21.5 ± 0.3	1.27 ± 0.01	44.0 ± 0.1	Passable
F2	0.24 ± 0.03	0.28 ± 0.01	23.7 ± 1.0	1.31 ± 0.02	42.0 ± 1.7	Passable
F3	0.27 ± 0.04	0.35 ± 0.01	11.1 ± 1.0	1.12 ± 0.01	34.2 ± 1.8	Good
F4	0.29 ± 0.01	0.34 ± 0.01	13.2 ± 0.8	1.15 ± 0.01	33.9 ± 1.1	Good
F5	0.27 ± 0.03	0.35 ± 0.01	27.1 ± 0.8	1.37 ± 0.01	50.4 ± 0.2	Poor
F6	0.26 ± 0.01	0.30 ± 0.02	13.9 ± 0.7	1.16 ± 0.01	36.5 ± 1.3	Good
FPO	0.20 ± 0.02	0.29 ± 0.01	30.8 ± 0.7	1.44 ± 0.01	53.3 ± 0.4	Poor
F7	0.18 ± 0.05	0.26 ± 0.02	30.1 ± 0.6	1.43 ± 0.01	53.7 ± 1.1	Poor
F8	0.22 ± 0.03	0.34 ± 0.04	31.1 ± 0.4	1.45 ± 0.01	53.0 ± 0.7	Poor
F9	0.21 ± 0.02	0.32 ± 0.01	37.5 ± 0.7	1.60 ± 0.02	60.3 ± 1.4	Very poor
FLO	0.29 ± 0.001	0.36 ± 0.01	18.3 ± 0.6	1.22 ± 0.01	37.5 ± 0.4	Fair
F10	0.14 ± 0.01	0.16 ± 0.02	13.1 ± 1.0	1.15 ± 0.01	33.9 ± 2.0	Good
F11	0.18 ± 0.05	0.21 ± 0.03	26.9 ± 0.5	1.37 ± 0.01	53.3 ± 1.1	Poor
FMO	0.11± 0.01	0.13 ± 0.02	13.7 ± 0.5	1.16 ± 0.01	34.7 ± 1.9	Good
Milled IBP	0.13 ± 0.03	0.17 ± 0.05	22.7 ±1.0	1.29 ± 0.02	41.8 ± 0.5	Passable

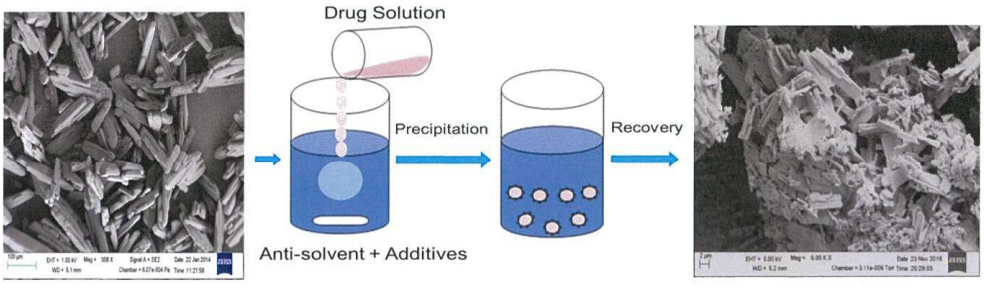
Drug Solution
Precipitation
Recovery
Anti-solvent + Additives
Raw IBP
Prepared IBP

Fig. 1.

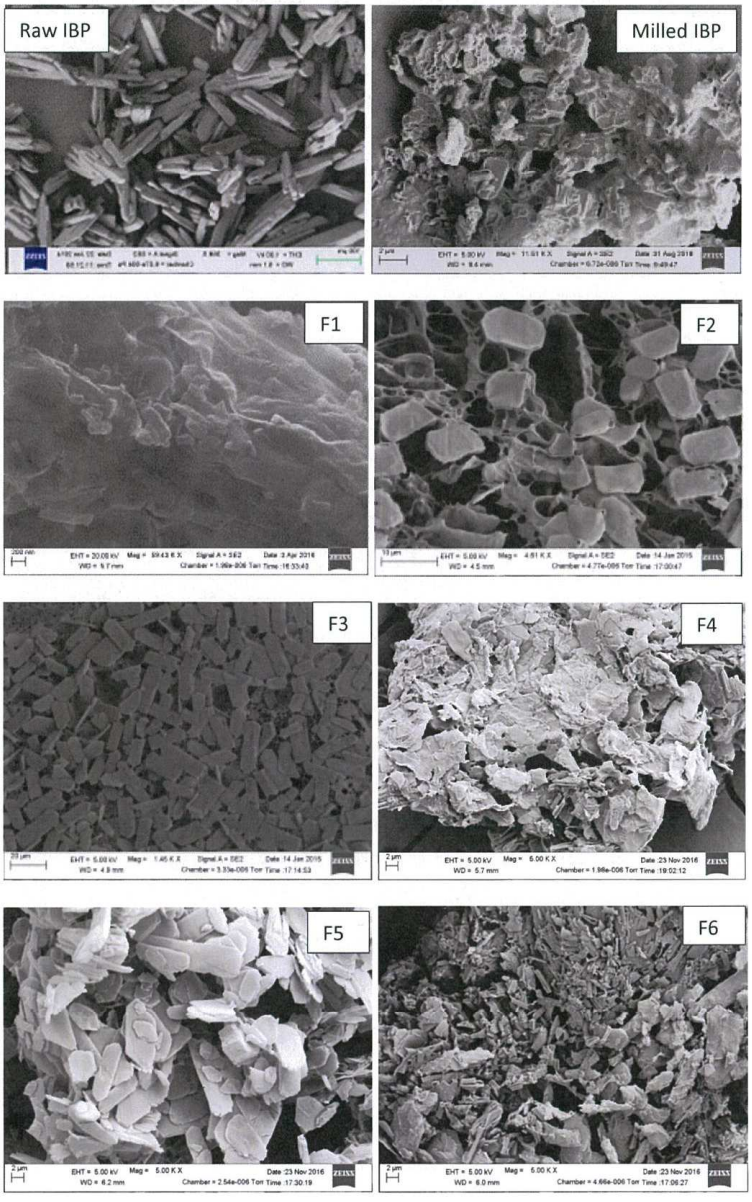
Raw IBP
Milled IBP
F1
F2
F3
F4
F5
F6

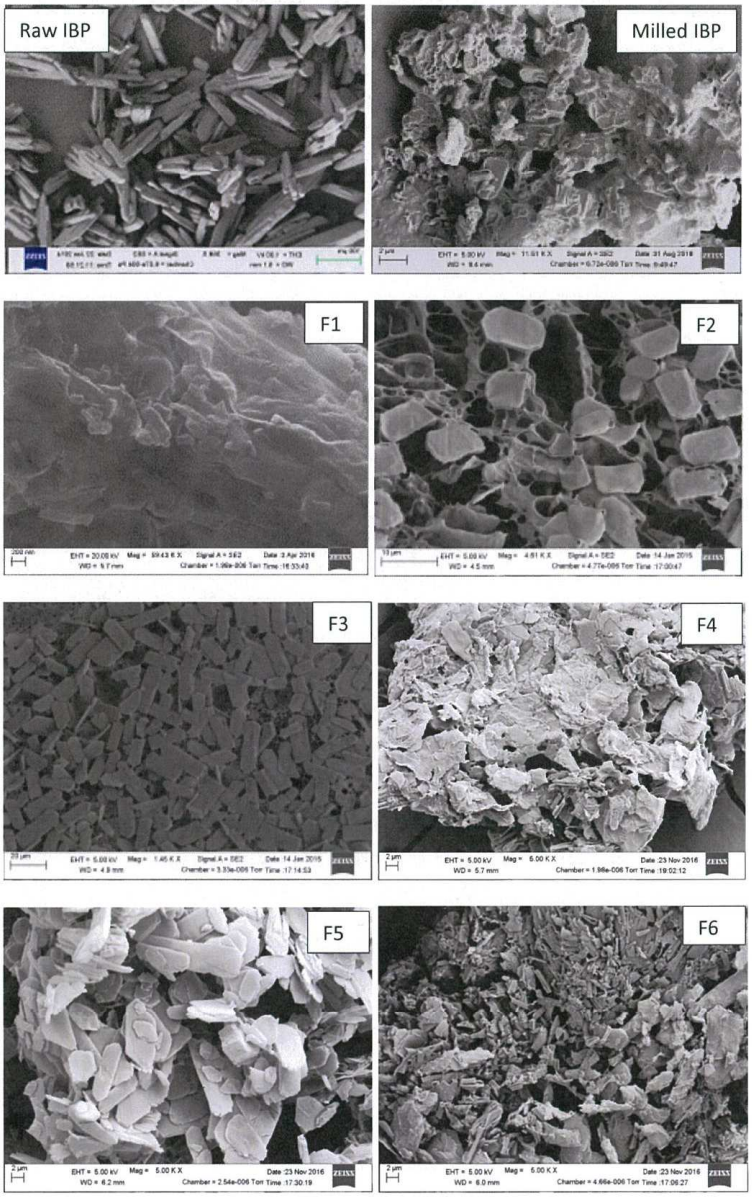
Raw IBP
Milled IBP
F1
F2
F3
F4
F5
F6

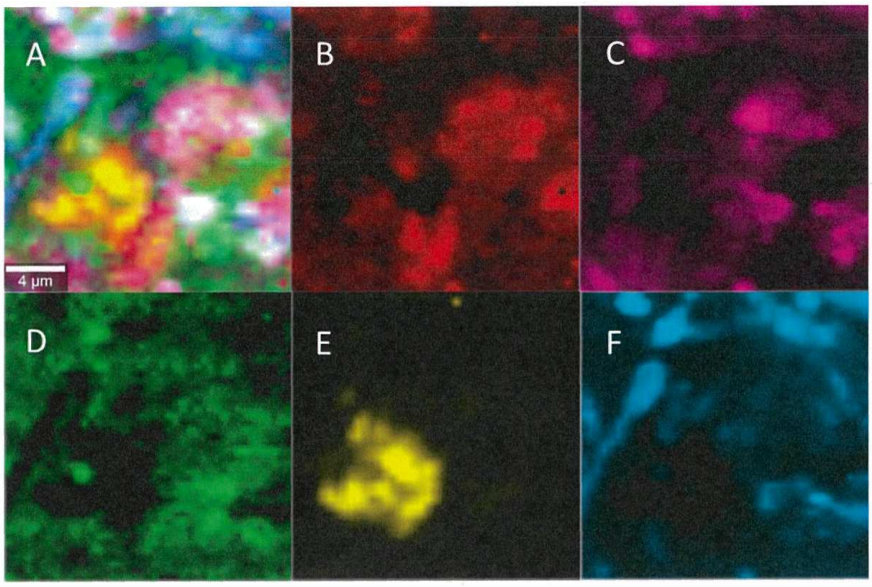

Fig.3.

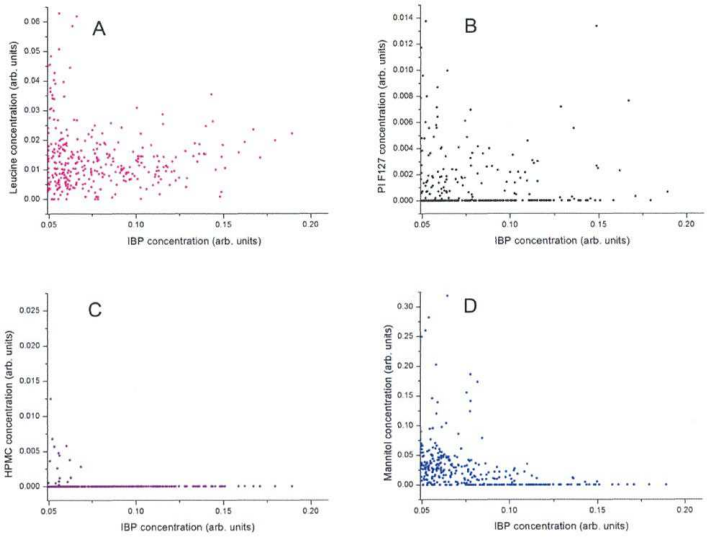
A
Leucine concentration (arb. units)
IBP concentration (arb. units)
B
PI F127 concentration (arb. units)
IBP concentration (arb. units)
C
HPMC concentration (arb. units)
IBP concentration (arb. units)
D
Mannitol concentration (arb. units)
IBP concentration (arb. units)

Fig. 4.

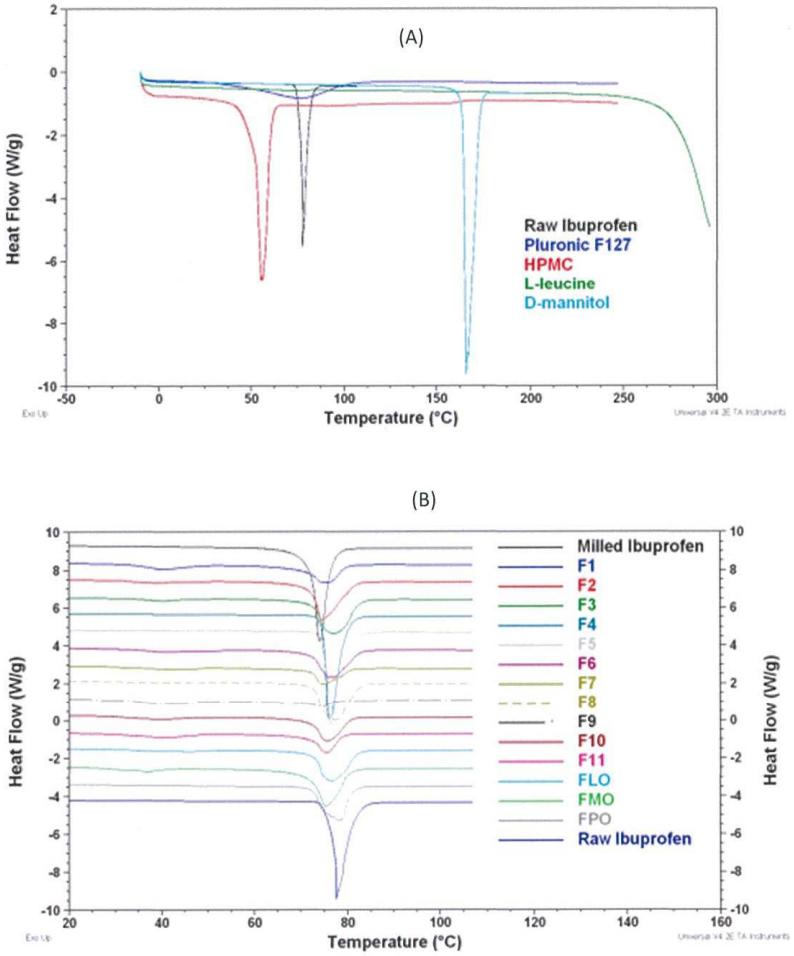
(A)
Heat Flow (W/g)
Temperature (°C)
Raw Ibuprofen
Pluronic F127
HPMC
L-leucine
D-mannitol
(B)
Heat Flow (W/g)
Temperature (°C)
Milled Ibuprofen
F1
F2
F3
F4
F5
F6
F7
F8
F9
F10
F11
FLO
FMO
FPO
Raw Ibuprofen

Fig. 5.

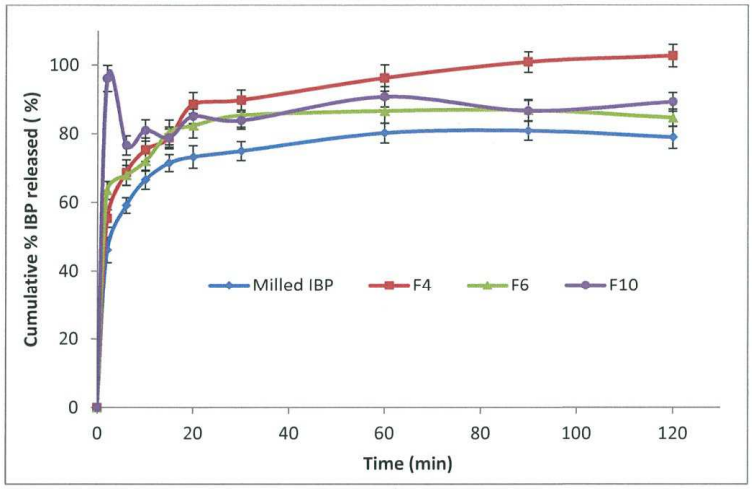
Cumulative % IBP released (%)
100
80
60
40
20
0
0
20
40
60
80
100
120
Time (min)
Milled IBP
F4
F6
F10

Fig. 6.